SAND2000-0345J

Thermal Stability of Electrodes in Lithium-Ion Cells

E. Peter Roth and Ganesan Nagasubramanian

Lithium Battery Research and Development Dept., Sandia National Laboratories, Albuquerque, NM, 87185-0613

Abstract

Differential scanning calorimetry (DSC) analysis was used to identify thermal reactions in Sony-type lithium-ion cells and to correlate these reactions with interactions of cell constituents and reaction products. An electrochemical half-cell was used to cycle the anode and cathode materials and to set the state-of-charge (SOC). Three temperature regions of interaction were identified and associated with the SOC (degree of Li intercalation) of the cell. Anodes were shown to undergo exothermic reactions as low as 80°C involving decomposition of the solid electrolyte interphase (SEI) layer. The $LiPF_6$ salt in the electrolyte (EC:PC:DEC/1M $LiPF_6$) was seen to play an essential role in this reaction. DSC analysis of the anodes from disassembled Sony cells showed similar behavior to the half-cell anodes with a strong exotherm beginning in the 80°C-90°C range. Exothermic reactions were also observed in the 200°C-300°C region between the intercalated lithium anodes, the $LiPF_6$ salt, and the PVDF binder. These reactions were followed by a high-temperature reaction region, 300°C-400°C, also involving the PVDF binder and the intercalated lithium anodes. Cathode exothermic reactions with the PVDF binder were observed above 200°C and increased with the SOC (decreasing Li content in the cathode). No thermal reactions were seen at lower temperatures suggesting that thermal runaway reactions in this type of cell are initiated at the anode. An Accelerating Rate Calorimeter (ARC) was used to perform measurements of thermal runaway on commercial Sony Li-ion cells as a function of SOC. The cells showed sustained thermal output as low as 80°C in agreement with the DSC observations of anode materials but the heating rate was strongly dependent on the SOC.

Sandia is a multiprogram laboratory operated by Sandia Corporation, a Lockheed Martin Company, for the United States Department of Energy under contract DE-AC04-94AL85000.

DISCLAIMER

Introduction

Lithium-ion cells have an advanced chemistry that exhibits superior performance characteristics to most other rechargeable battery systems. These cells are characterized by an intercalating carbon negative electrode, a metal oxide positive electrode and an organic liquid electrolyte. [1] Typical electrodes are prepared using a polymeric binder such as polyvinylidene fluoride (PVDF) and metallic current collector substrates (copper for anode, aluminum for cathode). At elevated temperatures, reactions can occur between the electrode materials, binder and electrolyte. These reactions can lead to cell degradation and possible thermal runaway. [2-5] Extensive work has been performed in understanding the thermal performance of the cell electrodes, particularly the anode structure. [6-17] The anode has been identified as a source of low temperature thermal reactions resulting from decomposition of the solid electrolyte interphase (SEI) layer which forms during the first Li intercalation of the anode carbon material. [7-8] The composition of this layer is complex and is determined by the exact composition of the electrolyte used. The major constituents of this layer have been shown to be Li_2CO_3, LiF, Li_2O and Li-alkylcarbonates. [11-13,15,18,19] Much of this layer is metastable and reacts with electrolyte HF impurities to form stable inorganic products such as LiF and other salts. [12,18,19] These HF impurities result from reaction of the $LiPF_6$ with low levels of water that are present in the solvent. This reaction occurs at temperatures even below 100°C and accelerates with increasing temperature

We have used Differential Scanning Calorimetry (DSC) to measure the thermal interactions between the electrode materials and the electrolyte as a function of the state-of-charge (SOC). Anodes and cathodes were cycled in a half-cell apparatus using Li counter and reference electrodes and set to different Li contents. Electrode materials were also obtained from disassembled commercial Sony US18650 lithium-ion cells for DSC analysis and comparison to the half-cell materials. In addition, we also used an accelerating rate calorimeter (ARC) to measure the thermal performance of complete Sony cells under adiabatic conditions at various states of charge. Understanding the fundamental reactions of these cell components is essential to describing and predicting the thermal behavior of the full cell and cell assemblies.

Experimental

In this work, cell materials corresponding to those used in the commercial Sony US18650 lithium-ion cell were investigated for thermal and chemical stability under charge/discharge conditions. The "as received" electrodes were initially received as sheets of current collector (aluminum for the cathode and copper for the anode) with coatings of active material on one or both sides. The Sony-type cells consist of Li_xCoO_2 as the active cathode material and MCMB 25-28 carbon (Osaka Gas, Japan) as the active anode material. Sheets of anode material of 70 μm thickness (9.4 mg/cm^2) were prepared on one side of 25 μm copper foil, while sheets of two-sided cathode material of 140 μm total thickness (18.9 mg/cm^2 per side) were prepared on 20 μm aluminum foil. KS-6 graphite (Lonza) (5 wt%) was added to the cathode oxide to increase conductivity. The anode films were prepared with 10 wt% PVDF as the binder, using N-methyl pyrrolidinone (NMP) as a solvent during the coating process while the cathode films

were prepared with 5 wt% PVDF. The electrolyte (EM Industries, Inc.) consisted of ethylene carbonate (EC): propylene carbonate (PC): diethyl carbonate (DEC) (1:1:2 by weight) with 1.0 M $LiPF_6$ as the salt.

The basic electrochemical reactions are:

Cathode $$Li_1CoO_2 \underset{\text{discharge}}{\overset{\text{charge}}{\rightleftarrows}} Li_{1-y}CoO_2 + yLi^+ + ye^- \quad (1)$$

Anode $$6\,C + yLi^+ + ye^- \rightleftarrows Li_yC_6 \quad (2)$$

Overall $$Li_{1.0}CoO_2 + 6C \rightleftarrows Li_yC_6 + Li_{1-y}CoO_2 \quad (3)$$

Referencing the degree of Li intercalation of either electrode as "x", the range of stability of the Li_xCoO_2 crystal structure limits the Li level of the cathode to about $x = 0.5$, giving a nominal composition of $Li_{0.5}CoO_2$ for the cathode in the fully charged cell. [20] The voltage of the cathode vs. Li/Li^+ is 4.1 V for the charged cell while that of the cathode in the discharged cell (Li_1CoO_2) is 3.0 V. The corresponding voltage of the anode vs. Li/Li^+ in the charged cell is ~0.0 V and 3.0 V in the discharged cell. The range of Li intercalated in the anode is nominally from $0.0 < x < 1.0$. The actual amount of Li in the carbon anode was not determined as a function of electrode voltage but we shall refer to the fully charged anode (Li_xC_6) as the x=1 charge state and to the discharged state as x=0.

The thermal stability of the electrode components was investigated using differential scanning calorimetry. The cell components were characterized singly and in various combinations. Particular attention was given to interactions of the cell materials separately with the solvent and the electrolyte. The "as received" electrode sheet materials were also measured with and without the presence of the electrolyte.

The electrodes were cycled using an electrochemical half-cell (T-cell) apparatus as shown in Figure 1. Discs of the electrode material (0.5 in. diameter) were cut from the electrode sheets and held by spring tension in the T-cell. Lithium foil was used as the counter and reference electrodes while EC: PC: DEC/1M $LiPF_6$ (1:1:2) was used as the electrolyte. The cells were cycled using an Arbin battery test system (Arbin Corp., College Station, Texas). Anodes were cycled repeatedly (at least five times) at low current rate (0.4 mA/cm^2) to allow for irreversible lithium uptake in the "as manufactured" electrodes. The cathodes were cycled in a similar manner. Only electrodes exhibiting near 100% charge/discharge coulombic efficiency were used for further analysis. After cycling, the electrodes were placed in a state of known charge (known Li content). The lithium levels were set by direct coulombic measurement using the coulombic capacity between maximum charge/discharge voltages as the reference for each electrode. The electrodes were then rinsed with DEC to remove the electrolyte and vacuum dried. These rinsed and dried electrodes were measured in the dry state, followed by measurement in the presence of the solvent, and finally measurement in the presence of the full solvent/salt electrolyte. DSC was performed using a DSC2920 (TA Instruments, New Castle, Delaware). Samples were loaded under dry, room air atmosphere and sealed in hermetic aluminum sample pans although these pans did not retain their hermeticity at high internal pressures. Measurements were performed from ambient temperature up to 400°C. The

decomposition of the electrolyte at elevated temperature results in the generation of gas products causing significant overpressure in the aluminum pans. The pans undergo an endothermic response in proportion to the rate of gas release. Measurements of the electrolyte components were made to characterize this thermal signature. Cycled electrodes were measured consisting of three small (0.125 in. dia.) discs punched out from the larger T-cell disc and sealed in the DSC Al pans either with or without liquid solvent/electrolyte. Some measurements were also made using high-pressure stainless steel pans up to 300°C to determine the intrinsic thermal behavior of the gas generating materials under constant volume conditions without the endothermic effects from pan venting.

Several Sony 18650 cells were measured using the ARC to determine the effects of state of charge and thermal history on the overall thermal performance and stability of the full cells. The ARC (ARC2000, Arthur D. Little Co., Cambridge, MA) was used to measure the cells from 25°C to 140°C at open circuit voltages corresponding to 0-100% SOC. The ARC allows measurement of self-heating reactions in the cell under adiabatic conditions. The ARC was programmed for 5°C temperature increments with a 20-min wait period and a 10-minute slope determination period. The heating rate threshold for determination of self-heating was set at 0.02°C/min.

Results and Discussion

Starting Materials-- The PVDF binder is a component of both the anode and cathode materials that can contribute to the thermal reactions in a cell. This binder material was measured in the DSC up to 400°C and then remeasured to determine irreversible changes. Figure 2 shows an endothermic peak at 175°C resulting from sample melting and some exothermic reactivity above 300°C. The repeat scan showed that the endothermic melt peak was reduced in magnitude indicating that some irreversible decomposition did occur at the high temperatures.

The $LiPF_6$ electrolyte salt is another source of thermal reactivity in the cell. Figure 3 shows the data from the DSC scan of this salt in both the hermetic sealed Al pan and in the stainless steel high-pressure pan. The data from both pans showed that the salt decomposes endothermically at 195°C. The initial products of this decomposition are reported to be LiF and gaseous PF_5. [21] FTIR analysis of the gas decomposition products found PF_5 as well as evidence of HF and a P-O bond containing species (probably a phosphorus oxyfluoride), both of which could result from interaction of the $LiPF_6$ with trace water. These escaping gaseous products from the Al pan produce an endothermic peak in the 200°C-275°C range. Separate thermal graviometric analysis (TGA) of the decomposing salt showed a close correlation between the DSC endotherm and the rate of mass loss, as shown in Figure 3. No further thermal reactions above the melt temperature were observed in the DSC high-pressure pan scan.

Figure 4 shows the DSC data for the full electrolyte solution in both the Al pan and the high-pressure pan. The data from the high-pressure pan show that the electrolyte decomposition reactions are exothermic. Gaseous products escaping from both the decomposition of the solvent and the salt produce a double endotherm that is the typical signature for DSC scans of electrolyte mixtures in the Al pans. This endotherm seen for the Al pan scan will be part of the thermal signature of any sample run with the electrolyte solution in the Al pans.

DSC scans of the uncycled anode and cathode materials with and without the presence of the electrolyte showed no thermal reactions over the full temperature range other than the electrolyte decomposition reaction. The anodes and cathodes were then cycled in the T-cell at 0.4 mA/cm^2 between voltages corresponding to known stability limits and composition of the active materials as mentioned earlier. After five conditioning charge/discharge cycles, the anode Li levels were set at x=0.0, 0.1, 0.3, 0.5, 0.7, 0.9 and 1.0 in Li_xC_6, and the cathode Li levels were set at x=0.5, 0.75 and 1.0 in Li_xCoO_2.

Cathodes-- The cycled cathode electrodes were removed from the T-cell, rinsed and dried as described previously. DSC measurements of these rinsed/dried samples are shown in Figure 5. Weak exothermic reactions were seen which increased in magnitude with decreasing Li content over a temperature range of 250°C-350°C. The addition of the EC:PC:DEC solvent resulted in significantly increased exothermic reactions for the cathodes with x=0.75 and x=0.5 Li levels as shown in Figure 6. The exotherms increased in magnitude and occurred at lower temperatures with the decreasing Li levels. However, the cathode for the fully discharged cell (x = 1.0) showed only the characteristic solvent endotherms. As seen in Figure 7, the cycled cathodes in the presence of the EC:PC:DEC/$LiPF_6$ electrolyte showed similar behavior. These measurements show that the x = 1.0 cathodes (discharged cell) exhibit no thermal activity over the entire temperature range, independent of solvent/electrolyte exposure while the cathodes with reduced Li level (charged cell) showed significantly enhanced exothermic reactions in the presence of the EC:PC:DEC solvent, independent of the presence of the $LiPF_6$ salt. We believe that the removal of the Li from the $LiCoO_2$ crystal structure, which results in an increase in the oxidation potential of the active material, results in enhanced solvent decomposition at the crystal/solvent interface, possibly including interaction with the PVDF polymer. Thus, the cathode contribution to thermal instability in the cell occurs after the cell has already reached high temperatures (>200°C) and is not of major concern for discharged cells.

Anodes-- The cycled anodes were removed from the T-cell, rinsed and dried as described earlier, and measured in the DSC in the same manner as for the cathodes. Figure 8 shows the DSC data up to 400°C for each Li level. Exothermic reactions were seen in the 250°C-400°C range for Li levels of 0.5 or greater. However, little or no thermal activity was seen for the 0.0 to 0.3 Li levels. The exotherms increased in magnitude with increasing Li content of 0.5 or greater, starting with a peak near 370°C and shifting to lower temperatures for the two highest Li levels. This activity suggests that the Li intercalated carbon is reacting directly with the PVDF. No thermal activity was seen for any of the rinsed/dried anodes at temperatures below 250°C. The effect of adding EC:PC:DEC solvent to the anodes is shown in Figure 9. No thermal activity was seen below 300°C for any Li level, other than the characteristic solvent endotherms. Above 300°C, exothermic reactions occurred only for Li levels of 0.5 or greater, increasing in magnitude with the Li content, as was seen for the rinsed and dried anodes. However, the exotherms were now broader with a peak around 375°C. This behavior is qualitatively similar to that seen in the rinsed and dried anodes, indicating that the solvent is not contributing significantly to this reaction.

The effects of adding the EC:PC:DEC/$LiPF_6$ electrolyte to the cycled anodes are shown in Figure 10. The thermal reactions are now much more complex. Significant exothermic reactions occurred in the low-temperature regime below 200°C, with double exotherms centered

around 100°C and 150°C. The magnitudes of the lower temperature peaks were not correlated with the Li levels. Repeat measurements showed similarly high peaks for Li levels of 0.1 and 0.7. The magnitude of the higher temperature peak was inversely related to the magnitude of the lower temperature peak. If the lower temperature peak was high, the higher temperature peak was low, and vice versa. This relationship suggests that the reaction in this temperature range involves the same materials and is limited by a fixed quantity reactant. Other work has attributed these reactions to an electrolyte/SEI layer interaction.[7-9] Metastable SEI layer components are believed to react with HF impurities originating from $LiPF_6$ reacting with trace water.[12,18,19] The metastable layer is converted to a stable inorganic layer until either the intercalated Li is consumed or the layer becomes too thick for Li diffusion. Our measurements substantiate this model since no reactions were observed for the uncycled anodes. The participation of the $LiPF_6$ in this SEI reaction, possibly through HF formation, is further indicated by the lack of reaction that was observed when only the solvent was present with the intercalated anodes. This SEI/$LiPF_6$ reaction can contribute significantly to the thermal runaway behavior of the cell. The thermal release beginning near or below 100°C can drive the cell temperature higher where further reactions can accelerate the temperature rise.

Increased exothermic activity was also seen in the 200°C-300°C intermediate-temperature regime for the anode/electrolyte sample. An exothermic reaction was superimposed on the solvent endotherms, increasing with increasing Li level and centered on 275°C. Because this behavior was not seen when solvent only was added to the anode, the $LiPF_6$ is again indicated as being involved in this exothermic reaction. We have shown that the solvent contributes to this exothermic reaction with the $LiPF_6$, but the Li dependence (charge state) indicates that reactions are occurring involving the intercalated Li and possibly the PVDF binder. The exact involvement of the $LiPF_6$ in this reaction is not known.

Exothermic reactions in the 300°C-400°C high-temperature regime were very similar to those seen for the solvent-only runs. Peaks near 375°C were seen only for the high Li level materials. This indicates that the $LiPF_6$ salt was not involved in these high-temperature reactions. Thus, these reactions were primarily Li/PVDF interactions.

The role of PVDF in these reactions was clarified in a set of measurements where the cycled anode films ($x = 1.0$) were first removed from the current collectors using NMP solvent. The PVDF dissolved in the NMP while the lithiated carbon remained as solid particles. The solid particles were removed by filtration and rinsed with DEC to remove the NMP. Electrolyte was added to the carbon particles, and the mixture was measured in the DSC like the earlier anode materials. As shown in Figure 11, a single exotherm was seen in the 125°C-175°C range. No exotherms were seen at lower temperatures, which previously had been associated with decomposition of the SEI layer. We believe that the absence of the low-temperature exotherms resulted from removal of part or the entire SEI layer by the NMP solvent. FTIR analysis of the NMP solutions showed the presence of Li_2CO_3, which is known to be a major constituent of the SEI layer. [11-13,15,18,19] The single remaining exotherm likely is the result of reaction of the remaining SEI components or solvent reduction by the Li-intercalated graphite. Also, no exothermic activity was observed either in the mid-temperature or high-temperature regimes. The only other thermal activity observed was the endotherm associated with venting from the

electrolyte decomposition gases. These measurements indicate that PVDF is essential to the higher temperature exothermic reactions above 200°C.

Sony Cells -- Commercial Sony US18650 cells were cycled and then disassembled in an argon glove box to separate the anode and cathode materials. The electrolyte from these cells was determined to be PC: DMC/$LiPF_6$. The anodes from two cells were measured straight from the cell without any rinsing, one cell in the fully charged state and the other cell in a nearly discharged state. The DSC data in Figure 12 show great similarity to data for the T-cell anodes prepared from the different electrolyte composition. A double exothermic reaction was measured in the 120°C-150°C range, although the reactions started slightly higher in temperature than seen in our previous measurements and were not well separated. No difference was seen between the charged and partially discharged anodes in this low-temperature regime. This result again indicates a SEI decomposition reaction. Exothermic reactions superimposed on the electrolyte venting endotherms were seen in the intermediate temperature range and continued into the high-temperature region. The fully charged anode material showed strong exothermic reaction in this high-temperature range while the partially discharged anode showed little reaction. This again is in good agreement with the behavior seen as a function of Li level in the T-cell anodes where these exotherms were shown to result primarily from Li/PVDF reactions.

Figure 13 shows the DSC data for the corresponding cathode materials removed straight from the cell. Again, we see behavior similar to that seen for the T-cell measurements shown in Figure 7. Exothermic reactions were seen in the 200°C-300°C range resulting from interactions between the Li_xCoO_2 active material, electrolyte and possibly PVDF. The figure shows that the more delithiated state (charged cell) resulted in higher thermal reactivity compared to the cathode from the partially discharged cell. However, new low-level exothermic activity was seen starting around 125°C and continuing up to 200°C. This activity looks similar to the SEI reactions seen in the anodes. It has been suggested that SEI products can possibly diffuse from the porous anodes to the cathodes in a full cell.[14] This would explain the absence of such reactions in the T-cell prepared cathodes which were run against Li metal which has much lower surface area for SEI layer formation. The magnitude of these reactions is still smaller than seen for the anode reactions.

Accelerating Rate Calorimetry -- Sony 18650 cells were cycled and set to 0%, 50%, 75%, 90% and 100% SOCs. Figure 14 shows the ARC data for these cells, which indicate that self-sustained heating was strongly dependent on the SOC. The charged cells exhibited self-heating as low as 50°C although accelerating heating rate was not seen until temperatures above 80°C. The low-temperature reactions were not self-sustaining and resulted from low-level discrete thermal events in the full cells. As the SOC decreased, the onset of accelerated heating shifted to higher temperature and the magnitude of the heating rate decreased. The fully discharged cell did not show accelerated heating until 130°C. For the fully charged cells, a "knee" in the heating rate was seen at about 110°C. This behavior is similar to that seen for the ARC runs of anode/electrolyte mixtures.[7,8] It was suggested that thermal reactions at the anode are transitioning from SEI metastable reactions to solvent reduction reactions by the intercalated anode. From the DSC measurements of the anodes and cathodes, it is believed that the anode SEI transformation results in the dominant source for cell heating, independent of the charge state (degree of lithiation). However, these ARC measurements indicate a strong dependence of the

anode reactions on cell voltage. These results are not surprising since lithium diffusion rates are dependent on the voltage gradient. [22]

After removal from the ARC, all cells were found to have undergone venting with the amount of electrolyte loss increasing with increasing SOC. Cell voltage was monitored during these ARC runs and showed a sudden decrease near 130°C. A decrease in the heating rate was observed for the charged cells near this same temperature. It is believed that cell venting and separator melting could account for this decrease in the heating rate and the drop in cell voltage. It is most interesting to note that after these events, the heating rate increased, even for the discharged cell. Thus, these safety features incorporated in the cell design do not limit thermal runaway under these open-circuit, thermally driven conditions.

A group of these Sony cells were exposed to additional aging over a range of time and temperature for comparison to the original cells. After aging, the thermal runaway performance was measured in the ARC as was done for the original cells. Figure 15 shows the data for an original cell, a cell aged at 25°C for 6 months, a cell aged at 60°C for 11 days and a cell aged at 70°C for 6 weeks. All cells were measured at 100% SOC. The data show that aging resulted in loss of the low-temperature heat output (heating rate below the 0.02°C/min ARC threshold) with increasing time and temperature. The onset of sustained heat output did not begin until 90°C for the 25°C/6 month cell, while the onset for the 60°C/11 day cell shifted up to 105°C and to 110°C for the 70°C/6 week cell. The cell heating rate responses showed the previously observed "knee" behavior in the 110°C-115°C range for all of the cells measured, although the onset of heating was much sharper for the cells aged at elevated temperature. These measurements suggest that the SEI layer is undergoing partial conversion from the metastable species to the stable inorganic species even at these low temperatures. The majority of this conversion takes place relatively quickly (less than two weeks) even at 60°C since little further change was noticed for the 70°C/6 week cell. The sudden increase in self-heating in the 100°C-110°C range suggests that the remaining SEI layer undergoes rapid conversion followed by further reaction of the lithiated anode with the electrolyte with increasing temperature. This rapid increase corresponds closely with the onset of the exothermic peak observed by DSC for these full-cell anodes.

Conclusion

The stability of Li-ion cathodes and anodes has been shown to be a complex function of constituent interactions and exposure conditions. Thermal analysis of the anodes and cathodes in these cells has shown that there are three regions of thermal activity. In the low-temperature regime (70°C-200°C), cycled anodes showed an exothermic SEI layer reaction that did not involve the PVDF binder. The magnitude of the exotherms did not correlate with the Li level. These reactions only occurred with the presence of $LiPF_6$ in the electrolyte and did not occur with only the EC:PC:DEC solvent.

In the intermediate temperature regime (200°C-300°C), the cycled anodes underwent an exothermic reaction (275°C) superimposed on the electrolyte endotherms, increasing in magnitude with increasing Li level. The reaction again only occurred with the presence of the

$LiPF_6$ in the electrolyte and did not occur for the pure solvent. This reaction is believed to be a Li/PVDF interaction not directly involving the solvent. Removal of the PVDF from the cycled films eliminated the reaction and confirmed that the PVDF is a main reactant.

In the high temperature regime (300°C-400°C), the cycled anodes showed increasing exotherms with increasing Li level only for Li levels 0.5 or greater. Those anodes with Li levels below 0.5 showed little or no thermal activity under any exposure conditions. These reactions occurred for the rinsed and dried films as well as in the presence of solvent or electrolyte. Removal of the PVDF from the films eliminated the exotherms. These results suggest that Li/PVDF is the most probable interaction occurring in this temperature range.

The cycled cathodes showed much less thermal activity at low temperatures than was seen for the anodes. Exothermic reactions only occurred in the 250°C to 350°C range and only for the cell states with $x < 1.0$. The cathodes for the fully discharged ($x = 1.0$) cells showed no thermal activity over the entire 70°C-400°C temperature range under any exposure conditions. The addition of solvent to the cathode films greatly enhanced the exothermic reactions, but no additional reactions were seen after the addition of the $LiPF_6$ salt. We believe that the removal of the Li from the $LiCoO_2$ crystal structure results in an increase in the oxidation potential of the structure, which results in enhanced solvent decomposition possibly including PVDF degradation.

ARC results showed that the onset of self-generated heating is a strong function of the cell voltage. Fully charged cells showed low-level thermal reactions as low as 50°C with the onset of accelerated heating around 80°C. Discharged cells only showed accelerated heating above 130°C after the cell had vented. Thermal runaway in these Li-ion cells initiates in the anodes involving the SEI layer reactions. Once the cell temperature reaches the 200°C range, the charged cathode contributes to the accelerating thermal reaction. Further exothermic reactions from the charged anodes reacting with the PVDF contribute to this runaway once these higher temperatures are reached. Aging was shown to reduce subsequent low-temperature reactions indicating that partial SEI transformation can occur even at temperatures below the threshold of detection by DSC. The increased cell voltage enhances these low-temperature reactions.

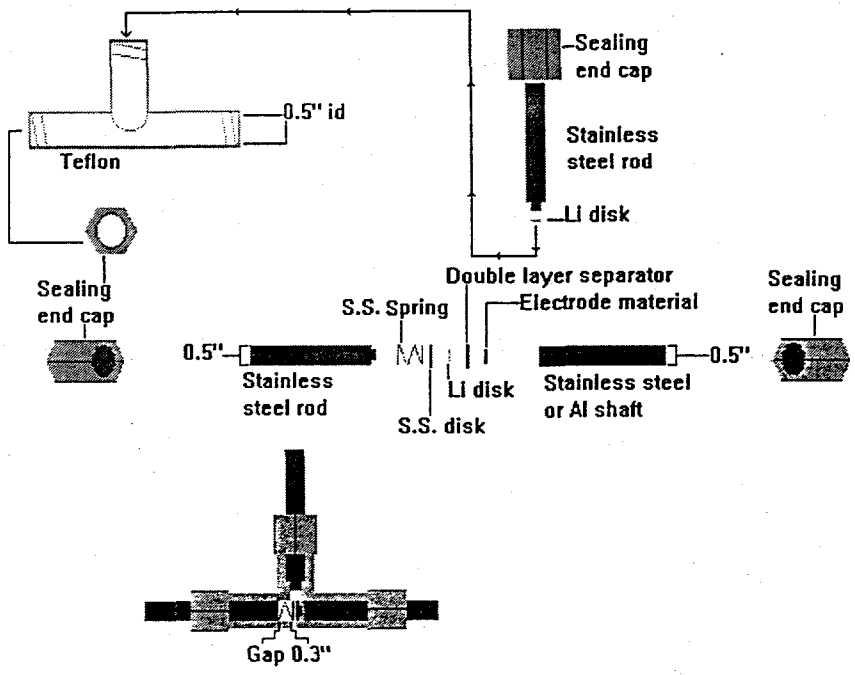

Figure 1. T-cell apparatus for cycling electrodes.

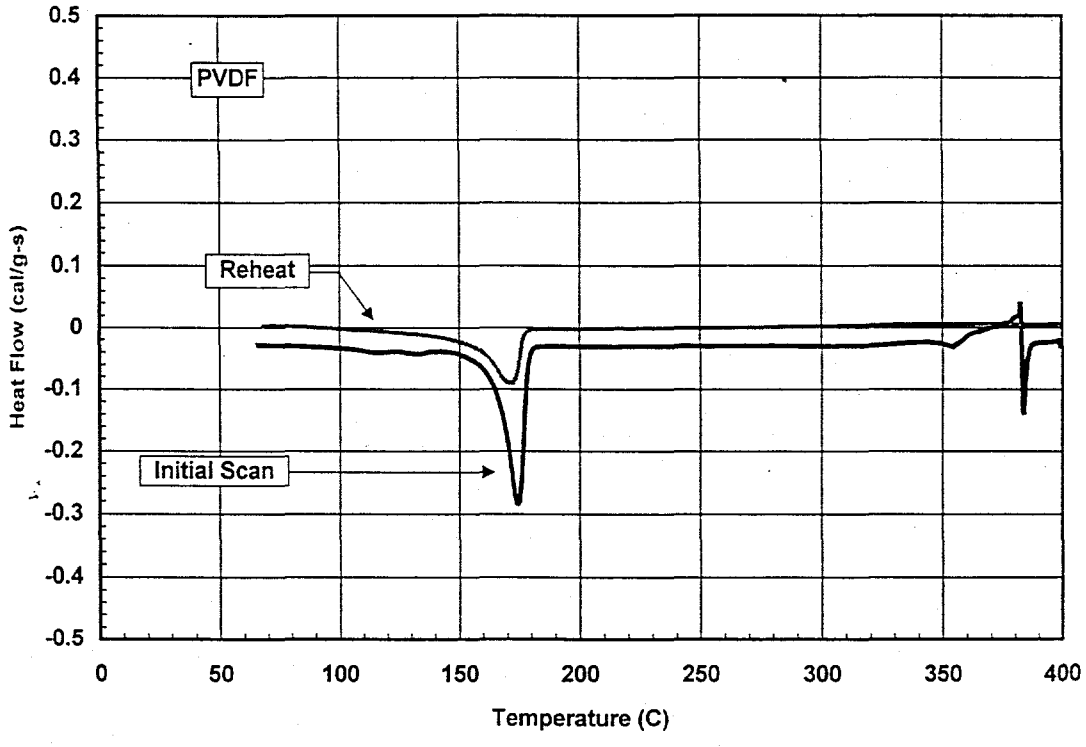

Figure 2. DSC scans of PVDF binder material.

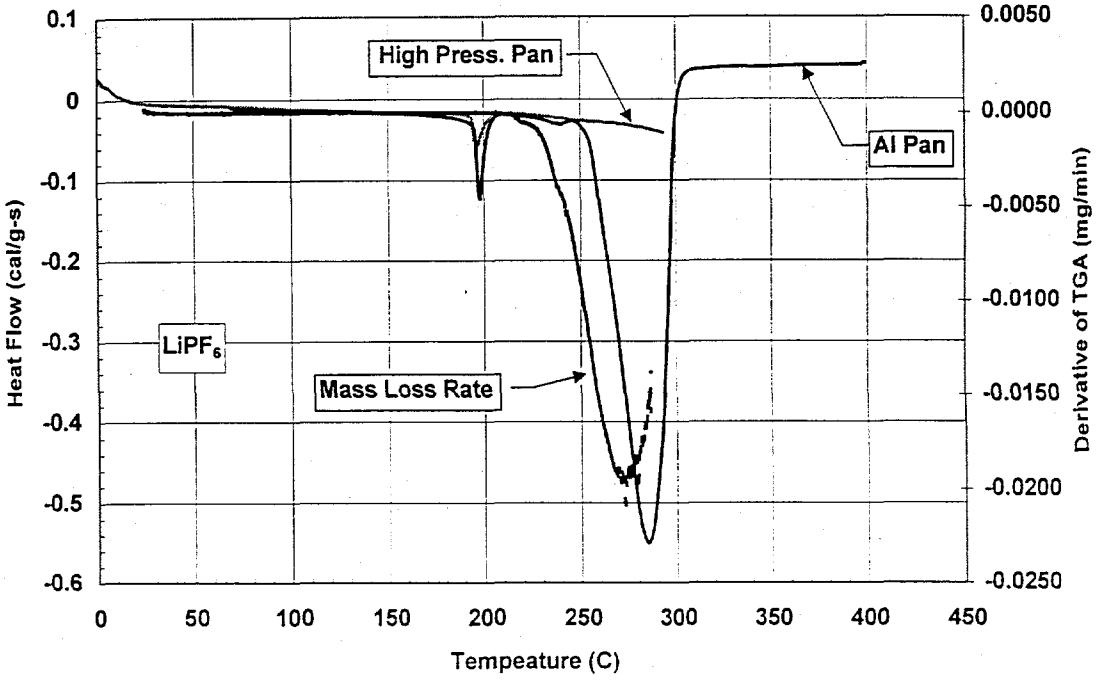

Figure 3. DSC scans of $LiPF_6$ salt in hermetic sealed Al pans and in high-pressure pans.

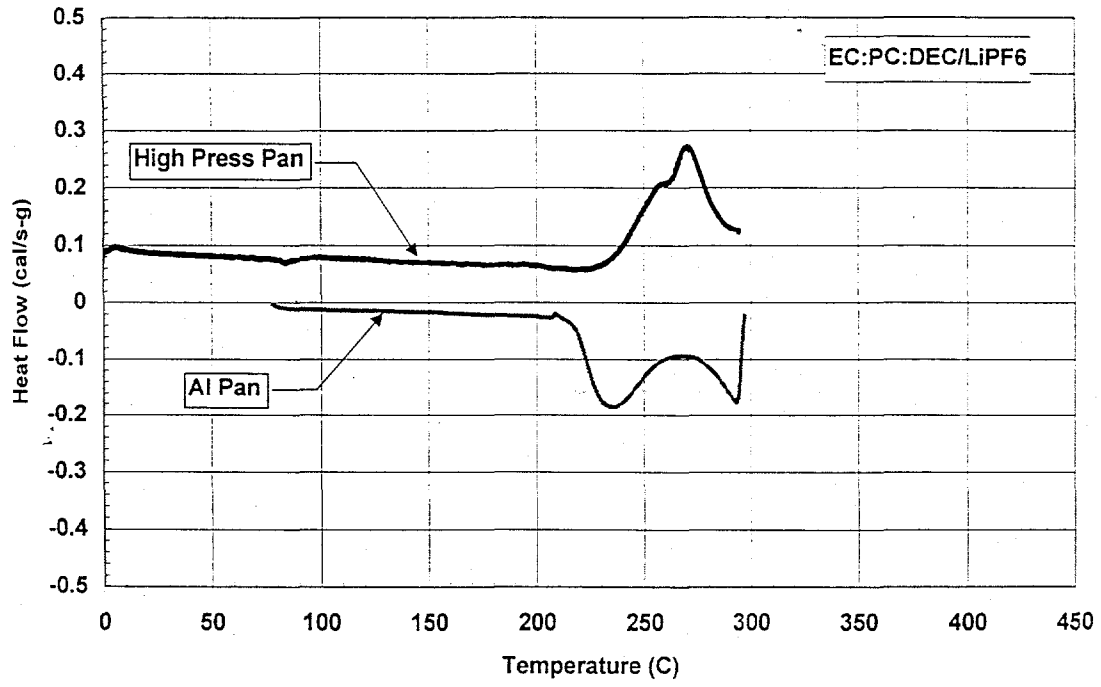

Figure 4. DSC scans of EC:PC:DEC/$LiPF_6$ electrolyte in hermetic Al pan and high-pressure pan.

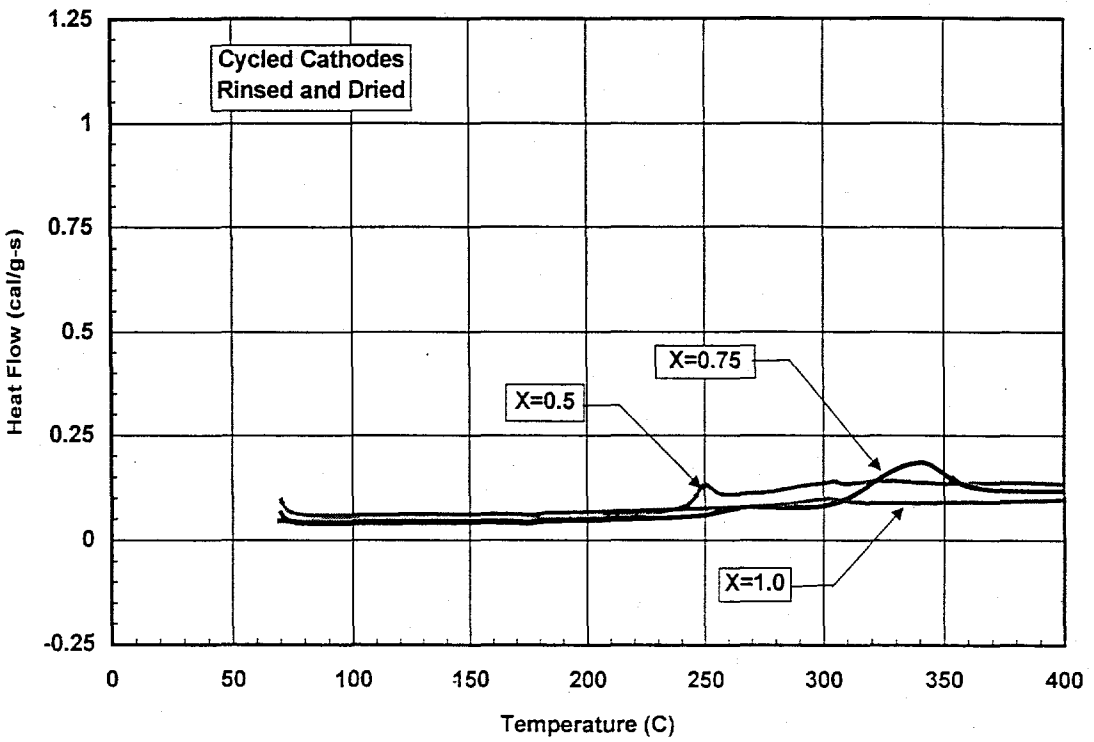

Figure 5. DSC scans of cycled cathode electrode rinsed/dried to remove electrolyte.

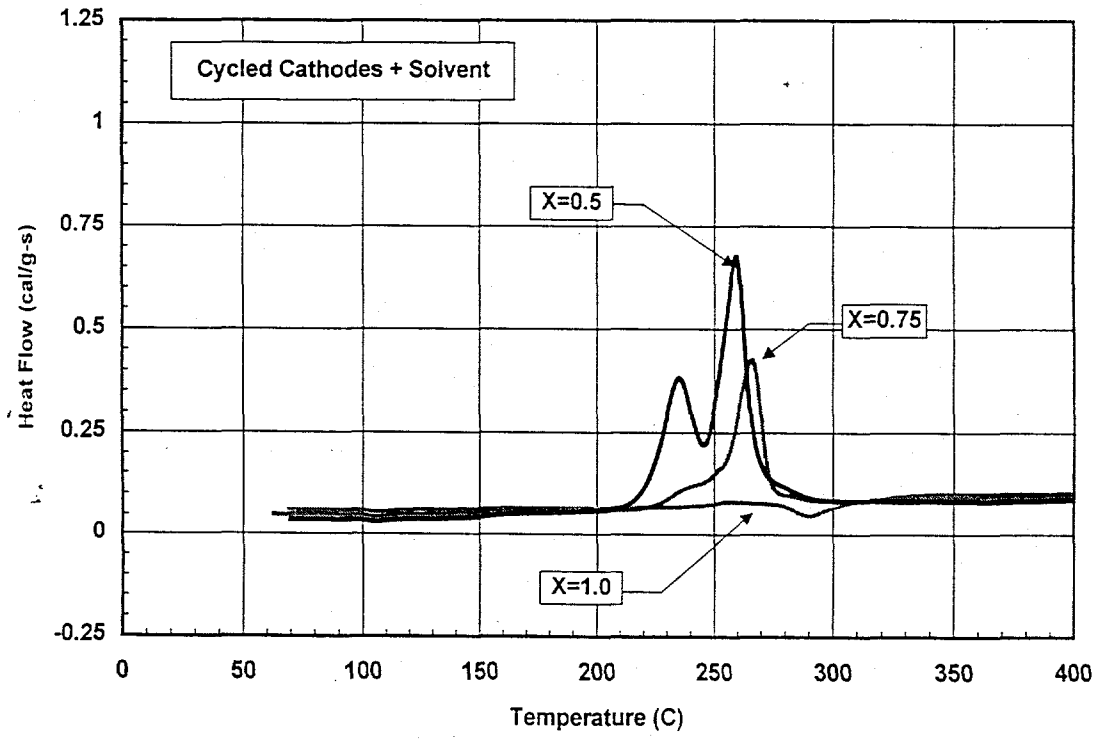

Figure 6. DSC scans of cycled cathode electrode: rinsed/dried, added solvent.

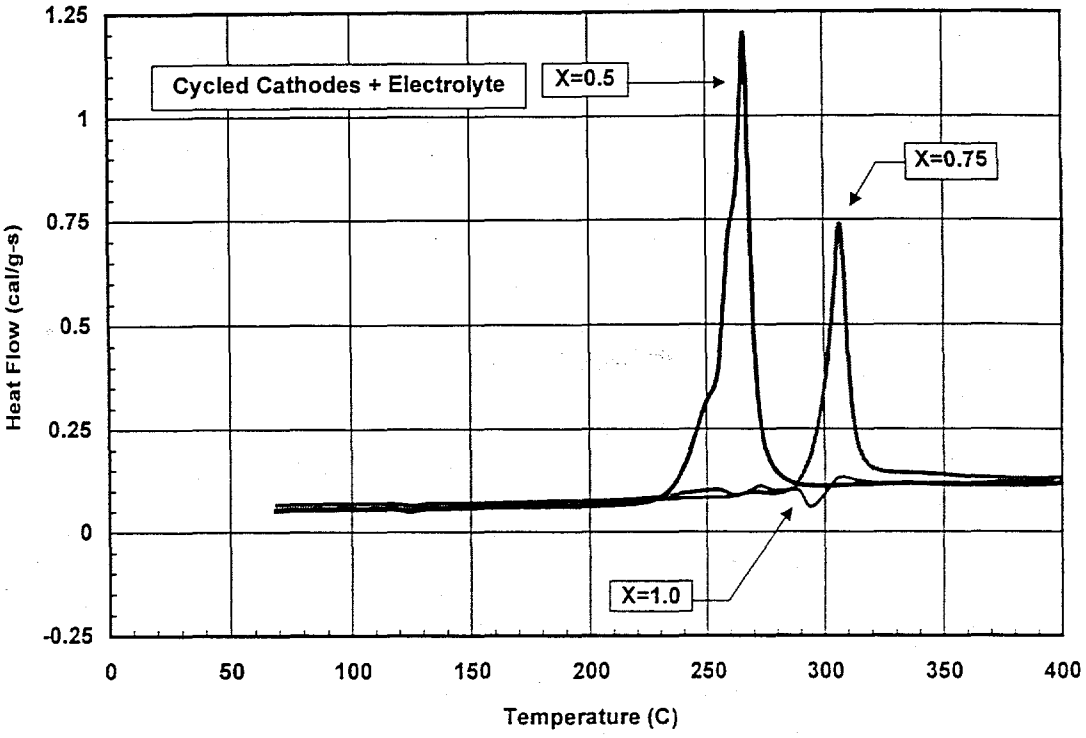

Figure 7. DSC scans of cycled cathode electrode: rinsed/dried, added electrolyte.

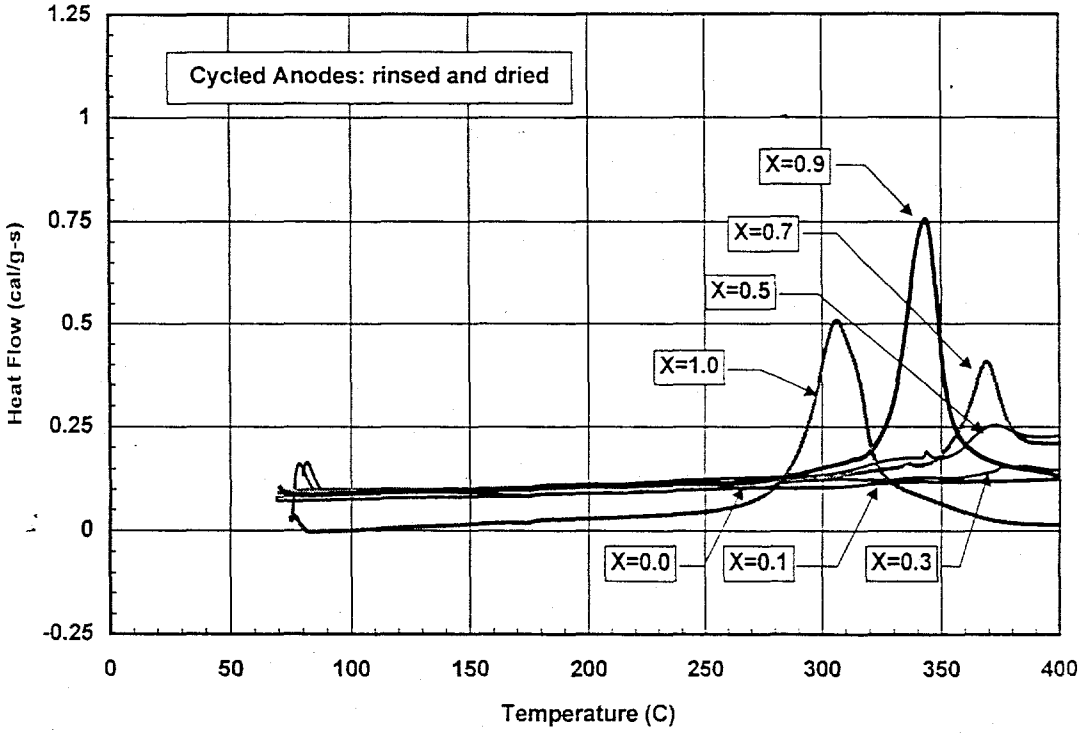

Figure 8. DSC scans of cycled anodes at increasing Li levels: rinsed/dried to remove electrolyte.

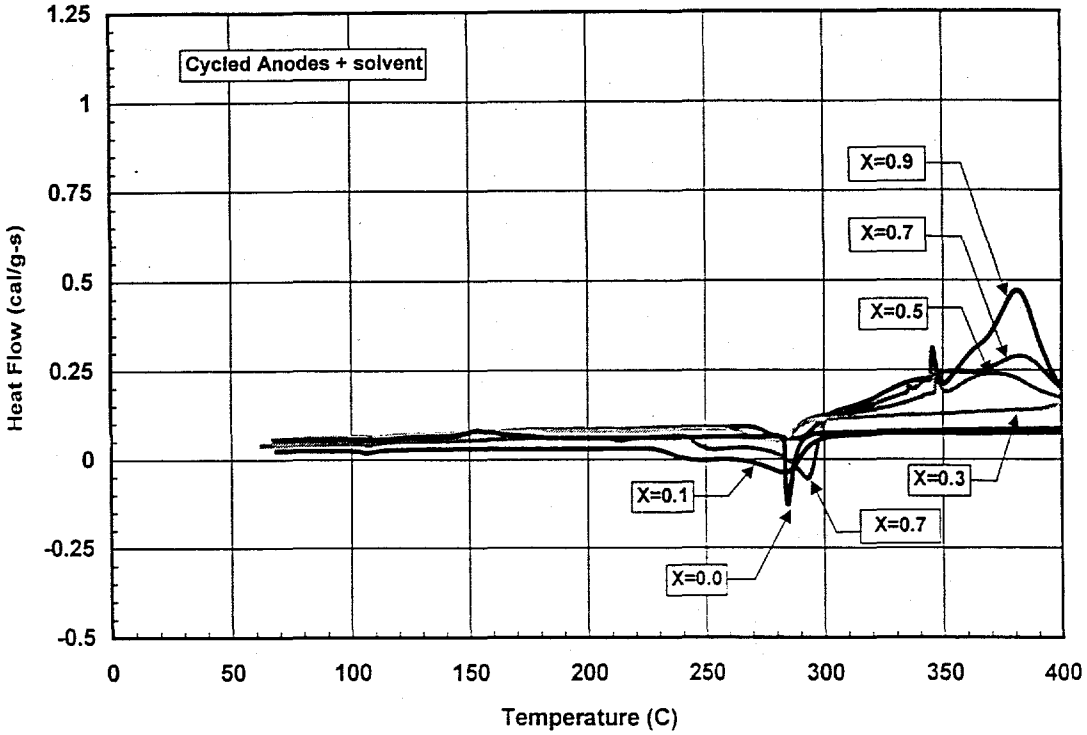

Figure 9. DSC scans of cycled anodes at increasing Li levels: rinsed/dried, added solvent.

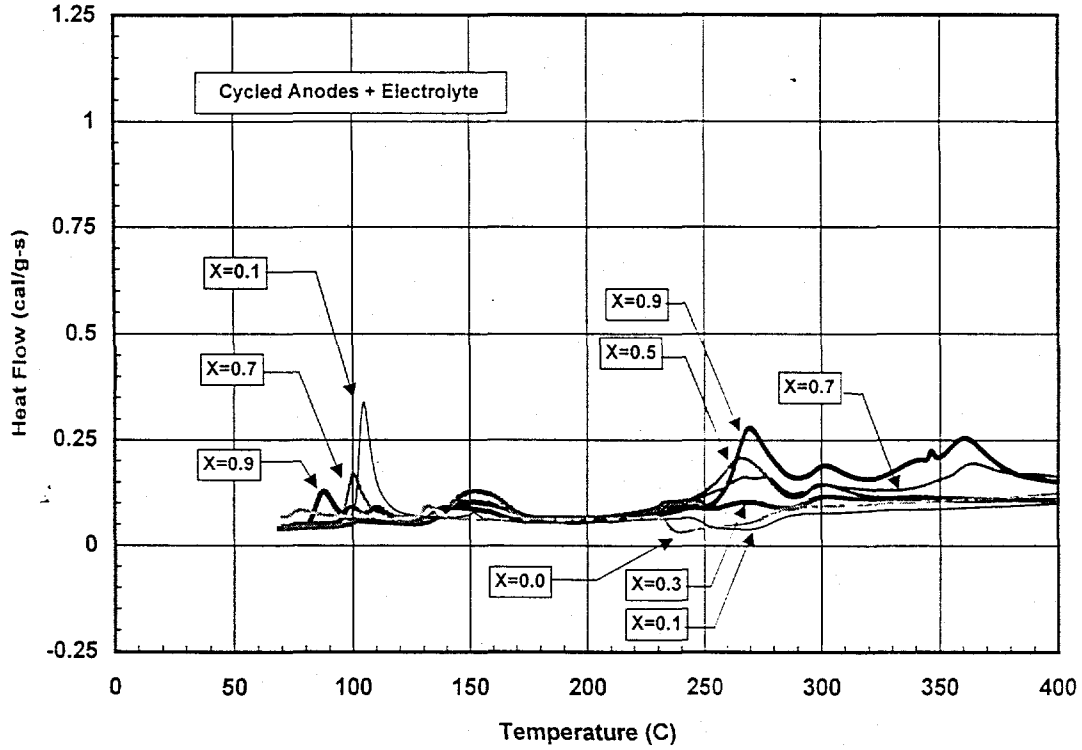

Figure 10. DSC scans of cycled anodes at increasing Li levels: rinsed/dried, added electrolyte.

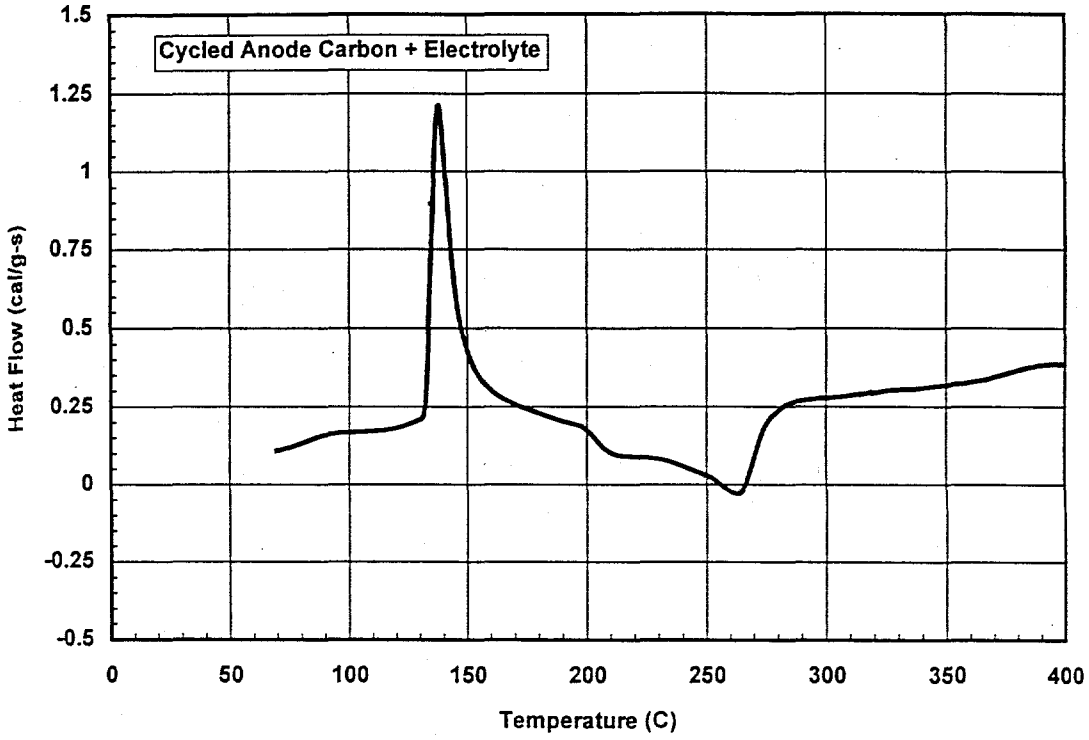

Figure 11. DSC scan of active carbon material from cycled anodes (x = 1.0) with PVDF removed.

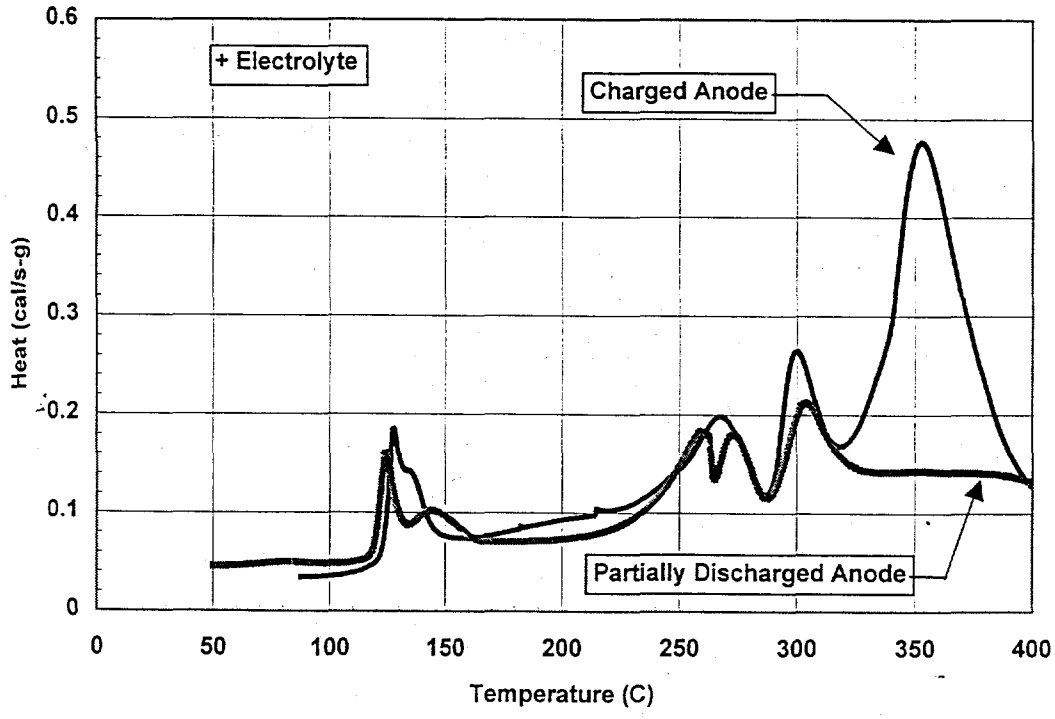

Figure 12. DSC data for anodes from disassembled Sony 18650 cells in charged and partially discharged state with electrolyte.

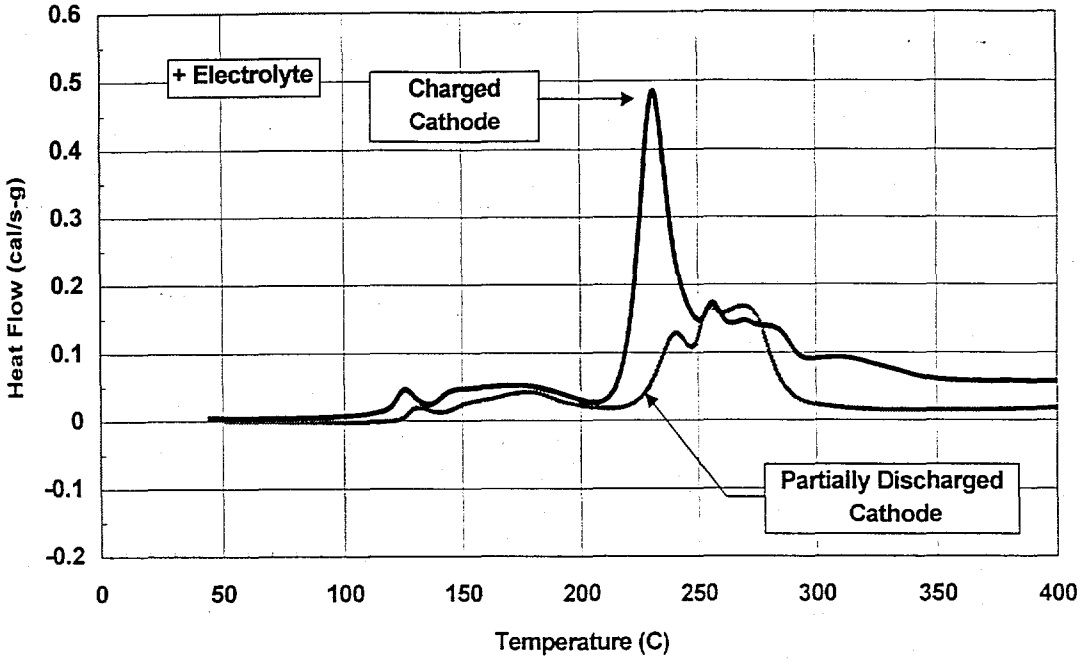

Figure 13. DSC data of cathodes from disassembled Sony 18650 cells, charged and partially discharged with electrolyte.

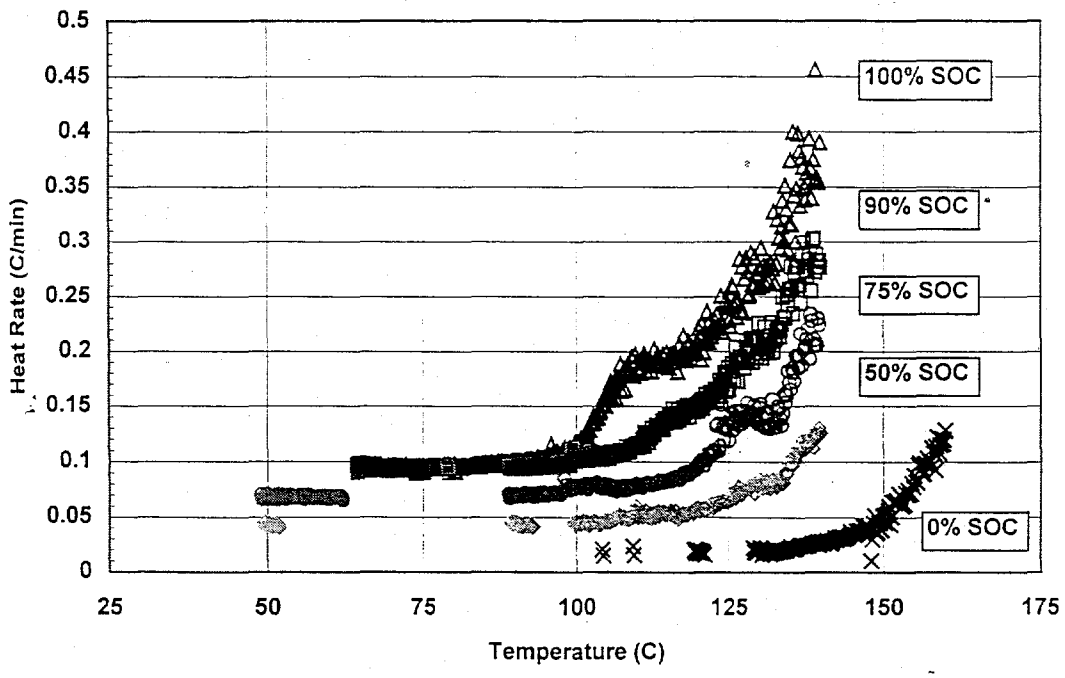

Figure 14. ARC data for Sony 18650 cells as a function of state of charge (vertically offset for clarity).

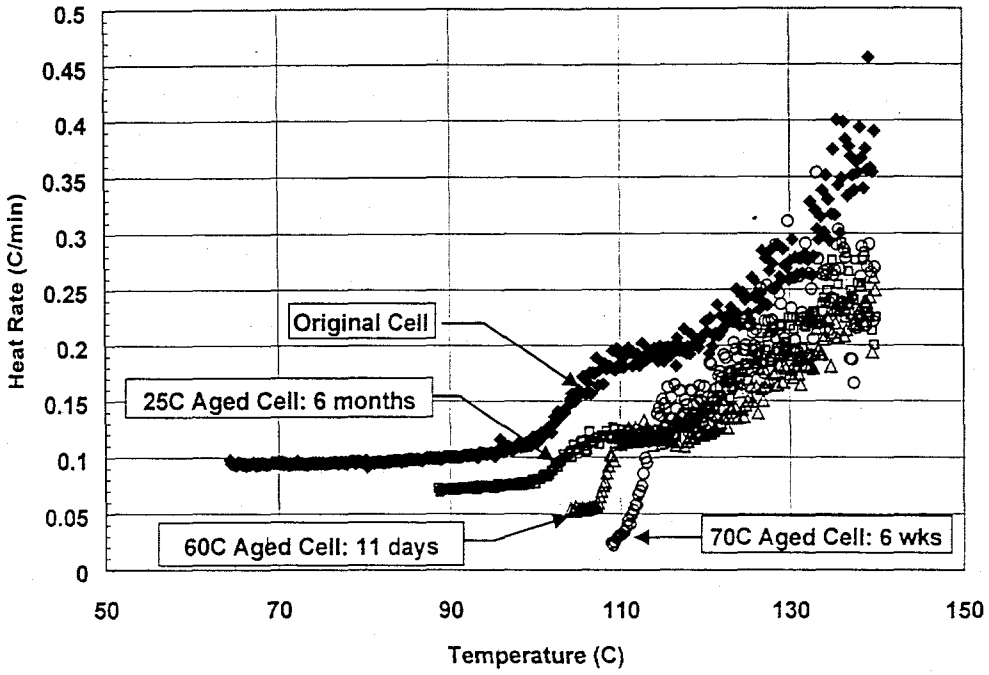

Figure 15. ARC data for thermally aged SONY 18650 cells at 100%SOC (vertically offset for clarity).

References

1. K. Ozawa, *Solid State Ionics*, **69**, 212 (1994).
2. H. Maleki, J. S. Hong, S. Al Hallaj and J. R. Selman, Abstract 128, p. 143, The Electrochemical Society and International Society of Electrochemistry Meeting Abstracts, Vol. 97-2, Paris, France, Aug. 31-Sept. 5, 1997.
3. J. Shi, C. Lampe-Onnerud, P. Ralbovsky, P. Onnerud, E. Carlson and B. Barnett, The Proceedings of the 194th Meeting of the Electrochemical Society, Vol. 98-16, p. 493-499, (1998).
4. C. Lampe-Onnerud, J. Shi, S. K. Singh, and B. Barnett, Proceedings of the Fourteenth Annual Battery Conference on Applications and Advances, p. 215-220, Long Beach, CA, Jan. 12-15, 1999.
5. J. Maleki, G. Deng, A. Anani, and J. Howard, *J. Electrochem. Soc.*, **146 (9)**, 3224-3229 (1999).
6. U. von Sacken, E. Nodwell, A. Sundher, and J. R. Dahn, *J. Power Sources*, **54**, 240-245 (1995).
7. M. N. Richard and J. R. Dahn, *J. Electrochem. Soc.*, **146 (6)**, 2068-2077 (1999).
8. M. N. Richard and J. R. Dahn, *J. Electrochem. Soc.*, **146 (6)**, 2078-2084 (1999).
9. M. N. Richard and J. R. Dahn, *J. Power Sources*, **79**, 135-142 (1999).
10. J. R. Dahn, E. W. Fuller, M. Obrovac, and U. von Sacken, *Solid State Ionics*, **69**, 265-270 (1994).
11. D. Aurbach, Y. Ein-Ely, and A. Zaban, *J. Electrochem. Soc.*, **141 (1)**, L1-L3 (1994).
12. D. Aurbach, A. Zaban, A. Schechter, Y. Ein-Eli, E. Zinigrad, and B. Markovsky, *J. Electrochem. Soc.*, **142 (9)**, 2873-2882 (1995).
13. D. Aurbach, Y. Ein-Eli, B. Markovsky, A. Zaban, S. Luski, Y. Carmeli, and H. Yamin, *J. Electrochem.l Soc.*, **142 (9)**, 2882-2889 (1995).
14. D. Aurbach, M. D. Levi, E. Levi, H. Teller, B. Markovsky, G. Salitra, U. Heider, and L. Heider, *J. Electrochem. Soc.*, **145 (9)**, 3024-3034 (1998).
15. E. Peled, D. Golodnitsky, C. Menachem, and D. Bar-Tow, *J. Electrochem. Soc.*, **145 (10)**, 3482-3486 (1998).
16. A. Du Pasquier, F. Disma, T. Bowmer, A. S. Gozdz, G. Amatucci, and J-M. Tarascon, *J. Electrochem. Soc.*, **145 (2)**, 472-477 (1998).
17. T. Zheng, A. S. Gozdz, and G. G. Amatucci, *J. Electrochem. Soc.*, **146 (11)**, 4014-4018 (1999).
18. Z. I. Takehara, Z. Ogumi, K. Kanamura, and Y. Uchimoto, in Lithium Batteries, N. Doddapaneni and A. R. Landgrebe, Editors, PV 94-4, p. 13-24, The Electrochemical Society Proceedings Series, Pennington, NJ (1994).
19. K. Kanamura, H. Tamura, S. Shiraishi, Z-I Takehara, *J. of Electroanalytical Chemistry,* **394**, p. 49-62 (1995).
20. J. N. Reimers and J. R. Dahn, *J. Electrochem. Soc.*, **139 (8)**, 2091-2096 (1998).
21. A. A. Smagin, V. A. Matyukha, and V. P. Korobtsev, *J. Power Sources*, **68**, 326-327 (1997).
22. T. F. Fuller, M. Doyle, and J. Newman, *J. Electrochem. Soc.*, **141 (4)**, 982-990 (1994).